

Journal of Visualized Experiments

Determining the Mechanical Strength of Ultra-Fine-Grained Metals

--Manuscript Draft--

Article Type:	Invited Methods Article - JoVE Produced Video
Manuscript Number:	JoVE61819R3
Full Title:	Determining the Mechanical Strength of Ultra-Fine-Grained Metals
Corresponding Author:	Bin Chen Center for High Pressure Science and Technology Advanced Research Shanghai, Shanghai CHINA
Corresponding Author's Institution:	Center for High Pressure Science and Technology Advanced Research
Corresponding Author E-Mail:	chenbin@hpstar.ac.cn
Order of Authors:	Jianing Xu Yanju Wang Jinyuan Yan Bin Chen
Additional Information:	
Question	Response
Please indicate whether this article will be Standard Access or Open Access.	Standard Access (US\$2,400)
Please indicate the city, state/province, and country where this article will be filmed . Please do not use abbreviations.	Berkeley, California, United States of America
Please confirm that you have read and agree to the terms and conditions of the author license agreement that applies below:	I agree to the Author License Agreement
Please specify the section of the submitted manuscript.	Engineering
Please indicate whether this article will be Standard Access or Open Access.	Standard Access (\$1400)
Please confirm that you have read and agree to the terms and conditions of the video release that applies below:	I agree to the Video Release
Please provide any comments to the journal here.	

Journal of Visualized Experiments
Editorial Office

July 2, 2020

Dear Editor:

We are submitting a manuscript entitled “Determining the mechanical strength of ultra-fine-grained metals” for your consideration as to its suitability for publication in Journal of Visualized Experiments. None of the material has been published or under consideration elsewhere, including the Internet.

The size dependence of strength of nanometals has been attracting a lot of interest. However, characterizing the strength of materials at the lower nanometer scale has been a big challenge as the traditional techniques (tension or indentation test, etc.) become no longer effective and reliable. Here we employ the radial diamond-anvil cell (rDAC) X-ray diffraction (XRD) techniques to track the change in differential stress and to determine the strength of ultrafine metals [Nature 579, 67-72 (2020)]. **This technique overcomes the limitation of the traditional methods.** Using this advanced technique, we observed ultrafine nickel particles have larger yield strength than coarser particles and size strengthening of nickel continues all the way down to 3 nm, extending the lower size limit of Hall-Petch relationship. We emphasize this technique to assess the mechanical performance of nanomaterials.

If you have any questions, please do not hesitate to contact us:

Tel: +86(21)80177063,

Fax: +86(21)80177064,

E-mail: chenbin@hpstar.ac.cn

Sincerely,

Bin Chen

Center for High Pressure Science & Technology Advanced Research, Shanghai, China

TITLE:

Determining the Mechanical Strength of Ultra-Fine-Grained Metals

AUTHORS AND AFFILIATIONS:

Jianing Xu^{1,2#}, Yanju Wang^{2#}, Jinyuan Yan³, Bin Chen^{1,2*}

¹School of Science, Harbin Institute of Technology, Shenzhen, China

²Center for High Pressure Science and Technology Advanced Research, Shanghai, China

³Advanced Light Source, Lawrence Berkeley National Lab, Berkeley, CA, USA

Email addresses of the authors:

Jianing Xu (xujianing@hit.edu.cn)

Yanju Wang (yanju.wang@hpstar.ac.cn)

Jinyuan Yan (jyan@lbl.gov)

Bin Chen (chenbin@hpstar.ac.cn)

*Email address of the corresponding author:

Bin Chen (chenbin@hpstar.ac.cn)

#These authors contributed equally

KEYWORDS:

High pressure, radial diamond anvil cell, X-ray diffraction, nanometals, mechanical strength, plastic deformation

SUMMARY:

The protocol presented here describes the high-pressure radial diamond-anvil-cell experiments and analyzing the related data, which are essential for obtaining the mechanical strength of the nanomaterials with a significant breakthrough to the traditional approach.

ABSTRACT:

The mechanical strengthening of metals is the long-standing challenge and popular topic of materials science in industries and academia. The size dependence of the strength of the nanometals has been attracting a lot of interest. However, characterizing the strength of materials at the lower nanometer scale has been a big challenge because the traditional techniques become no longer effective and reliable, such as nano-indentation, micropillar compression, tensile, etc. The current protocol employs radial diamond-anvil cell (rDAC) X-ray diffraction (XRD) techniques to track differential stress changes and determine the strength of ultrafine metals. It is found that ultrafine nickel particles have more significant yield strength than coarser particles, and the size strengthening of nickel continues down to 3 nm. This vital finding immensely depends on effective and reliable characterizing techniques. The rDAC XRD method is expected to play a significant role in studying and exploring nanomaterial mechanics.

INTRODUCTION:

The resistance to plastic deformation determines the materials' strength. The strength of the metals usually increases with the decreasing grain sizes. This size strengthening phenomenon can be well illustrated by the traditional Hall-Petch relationship theory from the millimeter down to submicron regime^{1,2}, which is based on the dislocation-mediated deformation mechanism of bulk-sized metals, i.e., dislocations pile up at grain boundaries (GBs) and hinder their motions, leading to the mechanical strengthening in metals^{3,4}.

In contrast, mechanical softening, often referred to as the inverse Hall-Petch relationship, has been reported for fine nanometals in the last two decades^{5–10}. Therefore, the strength of the nanometals is still puzzling as continuous hardening was detected for grain sizes down to ~10 nm^{11,12}, while the cases of size softening below 10 nm regime were also reported^{7–10}. The main difficulty or challenge for this debated topic is to make statistically reproducible measurements on the mechanical properties of ultrafine nanometals and establish a reliable correlation between the strength and grain size of the nanometals. Another part of the difficulty comes from the ambiguity in the plastic deformation mechanisms of the nanometals. Various defects or processes at nanoscale have been reported, including dislocations^{13,14}, deformation twinning^{15–17}, stacking faults^{15,18}, GB migration¹⁹, GB sliding^{5,6,20,21}, grain rotation^{22–24}, atomic bond parameters^{25–28}, etc. However, which one dominates the plastic deformation and thus determines the strength of nanometals is still unclear.

For these above issues, traditional approaches of mechanical strength examining, such as tensile test²⁹, Vickers hardness test^{30,31}, nano-indentation test³², micropillar compression^{33–35}, etc. are less effective because the high quality of large pieces of nanostructured materials is so difficult to fabricate and conventional indenter is much larger than single nanoparticle of materials (for the single-particle mechanics). In this study, we introduce radial DAC XRD techniques^{36–38} to material science to *in situ* track the yield stress and deformation texturing of nano nickel of various grain sizes, which are used in the geoscience field in previous studies. It has been found that the mechanical strengthening can be extended down to 3 nm, much smaller than the previously reported most substantial sizes of nanometals, which enlarges the regime of conventional Hall-Petch relationship, implying the significance of rDAC XRD techniques to material science.

PROTOCOL:

1. Sample preparation

1.1. Obtain 3 nm, 20 nm, 40 nm, 70 nm, 100 nm, 200 nm, and 500 nm nickel powder from commercial sources (see **Table of Materials**). The morphology characterization is shown in **Figure 1**.

1.2. Prepare 8 nm nickel particles by heating 3 nm nickel particles using a reaction kettle (see **Table of Materials**).

1.2.1. Put ~20 mL of absolute ethanol and ~50 mg of 3 nm nickel powder into the reaction kettle.

NOTE: The whole solution should not reach ~70% of the kettle volume.

1.2.2. Heat the reaction kettle at 80 °C for 24 h.

1.2.3. Cool the solution to room temperature and drop a little solution to one copper mesh (TEM grid, see **Table of Materials**).

1.2.4. Put the dried copper mesh into the Transmission Electron Microscopy (TEM) chamber and observe the sample morphology under 200 kV voltage electron beam.

NOTE: The copper mesh was air-dried for ~5 min or used a drying light of 5 min.

1.2.5. Measure the particle size distribution from the TEM images manually.

NOTE: The particle size measurement can also be done using any freely available software such as Image J.

1.2.6. Take out the solution and vaporize the ethanol at room temperature; then, the rest of the black solid is the pure nickel powder with an average particle size of 8 nm.

1.3. Prepare 12 nm nickel powder

1.3.1. Repeat step 1.2, but change the "absolute ethanol" and "80 °C for 24 h" to "absolute isopropanol" and "150 °C for 12 h" to obtain the pure nickel powder with the average particle of 12 nm.

2. High-pressure radial DAC XRD measurements

2.1. Make X-ray transparent boron-epoxy gasket utilizing a laser drilling machine (see **Table of Materials**).

2.1.1. Prepare Kapton (a kind of plastic) supporting gaskets

NOTE: Kapton is a polyimide film material (see **Table of Materials**).

2.1.1.1. Cut the inner circle with a laser drilling machine using the mentioned parameters: 35% laser power, three passes, 0.4 mm/s (cutting speed).

2.1.1.2. Cut the outer rectangular using the parameters: 80% of laser power, two passes, 1.2 mm/s (cutting speed). The rectangular dimension is 8 x 1.4 mm.

2.1.2. Prepare boron-epoxy gaskets from a larger boron disc with a diameter of ~10 mm.

NOTE: The boron disc is made by compressing the mixture of amorphous boron powder and

epoxy glue³⁶.

2.1.2.1. Polish the raw discs to a thickness of 60–100 μm with sandpaper manually.

NOTE: The sandpaper is from ~ 400 mesh to ~ 1000 mesh.

2.1.2.2. Cut the inner circles with a laser drilling machine using the mentioned parameters: 35% laser power, three passes, 0.4 mm/s (cutting speed).

2.1.2.3. Cut the outer circle with a laser drilling machine: 30% of laser power, one pass, 0.4 mm/s (cutting speed). Repeat and stop immediately when it comes off.

2.1.3. Assemble the gaskets

2.1.3.1. Place a Kapton supporting gasket (prepared in step 2.1.1) on a glass slide.

2.1.3.2. Place a drilled boron gasket on the inner hole of the Kapton gasket. Ensure that the larger end of the boron gasket is at the top.

2.1.3.3. Put another clean glass slide on the top. Hold it firmly and press it till the gasket is firmly inserted in the hole of Kapton gasket.

2.1.3.4. Store the fabricated gasket assemblies between two clean glass slides and wrap them with glue tape for future use.

NOTE: The gasket diameter, \varnothing = diamond culet size + 150 μm . For better reproducibility, the same setups can be used (possibly with small adjustments if something is found wrong) for the laser drilling and cutting during the gasket preparation. For good size matching, the diameter of gaskets entered for laser cutting is $\varnothing + 23 \mu\text{m}$ while the diameter of the inner hole of the Kapton supporting gaskets (entered for laser cutting) is $\varnothing - 23 \mu\text{m}$.

2.2. Radial DAC experiment loading

2.2.1. Mount the gasket assembly

2.2.1.1. On the viewing computer monitor (connected to the optical microscope), mark a dot to locate the center of the diamond (the piston diamond of the DAC).

2.2.1.2. Mount the boron-epoxy gasket (prepared in step 2.1) and the mark at the center of the gasket hole.

2.2.1.3. Use a glass slide to press down the gasket assembly such that the gasket firmly sets on the diamond of the piston.

NOTE: A DAC has two identical pieces of diamonds. Generally, the upper one is called cylinder diamond, and the lower one is called piston diamond.

2.2.2. Cleaning and compacting the gasket setup

2.2.2.1. Load samples with a chunk size smaller than the gasket hole such that there is no overflow of materials on the gasket surface.

NOTE: The samples here mean the candidate materials that we studied in our experiments. In this study, the samples are different-sized Ni powders and Pt chips.

2.2.2.2. Close the cell after the loading of a new piece of sample to achieve compactness.

2.2.3. Loading of soft materials (such as gold)

2.2.3.1. Load only one piece of the soft sample (make the soft material as a small fraction of the loaded materials).

2.2.3.2. Use hard amorphous materials to fill up the gasket hole for good compactness.

2.2.4. Loading of low atomic number materials (such as spinel, pyrope, serpentine)

2.2.4.1. Mix the sample with 10% Pt or Au. Fill up the gasket hole with the mixture but without overflow.

2.2.4.2. If necessary, put hard amorphous materials on the top for good compactness.

2.3. X-ray diffraction study

2.3.1. Mount the X-ray transparent boron-Kapton gasket (prepared in step 2.1) with a thickness of 100 μm and a chamber hole of 60 μm on the top of 300 μm culet of DAC with the support of the clays.

2.3.2. Place a small piece of Pt chip on top of the Ni sample as a pressure calibrant.

NOTE: No pressure medium was used to maximize the differential stress between the axial and radial.

2.3.3. Use a monochromatic synchrotron X-ray (see **Table of Materials**) with an energy of 25 or 30 keV to conduct the x-ray diffraction experiments.

2.3.4. Focus the X-ray beam to $\sim 30 \times 30 \mu\text{m}^2$ surface area on the sample.

2.3.5. Collect the X-ray diffraction patterns at pressure intervals of 1–2 GPa by a two-dimension

image plate (see **Table of Materials**) with a resolution of 100 $\mu\text{m}/\text{pixel}$. The setup used is shown in **Figure 2** and **Figure 3**.

2.4. The experimental data analysis

2.4.1. Process each X-ray diffraction image into a file containing 72 spectra over 5° azimuthal steps using Fit2d³⁷⁻⁴².

NOTE: A two-dimensional diffraction image contains 360° information. To analyze the stress and texture information, it is needed to separate into 72 files with 5° azimuthal information contained in each one. Fit2d is the software used to analyze X-ray diffraction data³⁷⁻⁴².

2.4.2. Refine the diffraction pattern with the Rietveld method in the MAUD³⁷ software. The lattice strain of each lattice plane was obtained by fitting the pattern^{37,40}.

2.4.3. Calculate the differential stress and yield strength according to the lattice strain theory³⁸ and von Mises yield criterion^{38,39} following step 2.5.

2.5. The lattice strain theory for the experimental data analysis

2.5.1. Determine the differential stress (the difference between these maximum ($\sigma_{22} = \sigma_{33}$) and minimum stress (σ_{11}) components) that provides a lower-bound estimate of a material's yield strength³⁸, σ_y , based on the von Mises yield criterion following equation (1)³⁸:

$$(1) \quad t = \sigma_{11} - \sigma_{33} < 2\tau = \sigma_y.$$

2.5.2. Obtain the direction-dependent deviatoric strain Q_{hkl} by measuring the d-spacings from different diffraction directions by following equation (2)³⁸:

$$(2) \quad Q_{hkl} = (d_{0^\circ} - d_{90^\circ}) / (d_{0^\circ} + 2d_{90^\circ}),$$

where d_{0° and d_{90° are the d-spacings measured from $\Psi = 0^\circ$ and $\Psi = 90^\circ$ (the angle between the diffraction vector and load axis), respectively.

2.5.3. Then, derive the value of t using equation (3)³⁸:

$$(3) \quad t = \frac{3Q_{hkl}}{\alpha[(2G_R(hkl))^{-1}] + (1-\alpha)(2G_V)^{-1}}, \text{ where } G_R(hkl) \text{ and } G_V \text{ are the shear modulus of the aggregates under the Reuss (iso-stress) condition and Voigt (iso-strain) condition, respectively; } \alpha \text{ is the factor to determine the relative weight of Reuss and Voigt conditions}^{40}.$$

NOTE: Considering the current experiments' complicated stress/strain conditions, $\alpha = 0.5$ is used in this study.

2.5.4. For a cubic system, calculate $G_R(hkl)$ and G_V as follows using equations 4-6^{38,40,41}:

$$(4) \quad [2G_R^X(hkl)]^{-1} = \left[S_{11} - S_{12} - 3(S_{11} - S_{12} - \frac{1}{2}S_{44})\Gamma(hkl) \right]$$

$$(5) \quad \Gamma(hkl) = (h^2k^2 + k^2l^2 + l^2h^2) / (h^2 + k^2 + l^2)^2$$

$$(6) (2G_V)^{-1} = \frac{5}{2} \frac{(S_{11}-S_{12})S_{44}}{[3(S_{11}-S_{12})+S_{44}]}$$

where S_{ij} are the single crystal elastic compliances and can be obtained from the elastic stiffness constants C_{ij} of materials.

3. TEM measurements

3.1. Prepare thin pressurized Ni foils for TEM using a focused ion beam (FIB) system (see **Table of Materials**). To reduce possible artifacts during ion milling of the specimen, deposit a protective Pt layer using the Pt gun equipped in the SEM with a thickness of $\sim 1 \mu\text{m}$ on the candidate region.

3.2. Perform TEM measurements on a 300 kV aberration-corrected transmission electron microscope equipped with high angle annular dark-field (HAADF) and bright-field (BF) detectors.

3.3. Take high-resolution TEM images.

REPRESENTATIVE RESULTS:

Under hydrostatic compression, unrolled X-ray diffraction lines should be straight, not curved. However, under non-hydrostatic pressure, the curvature (ellipticity of the XRD rings, which translates into the non-linearity of the lines plotted along the azimuth angle) significantly increases ultrafine-grained-nickel at similar pressures (**Figure 4**). At a similar pressure, the differential strain of the 3 nm sized nickel is the highest. The mechanical strength results (stress-strain curves) are shown in **Figure 5**. The strength continuously increases from coarser grains to finer grains, which is different from traditional knowledge^{5,6,10} (inverse Hall-Petch relationship). After complete yield, the nano metals also have strong strain hardening.

The *in situ* captured deformation texture of nano nickel with various grain sizes at different pressures can also be obtained from the radial DAC XRD data³⁶. In our previous study³⁶, larger nano grain sizes above 20 nm show very strong deformation texture even at low pressure. With grain size decreased below 20 nm, they show very weak deformation texture. It indicates that traditional total dislocation activity becomes less active in nano nickel below 20 nm. Naturally, other deformation mechanisms should take over the role of strengthening ultrafine nickel nanocrystals instead of the full dislocation slip.

To verify the partial slip deformation mechanism, TEM imaging measurements were conducted on the pressurized nickel crystals. As expected, high content of dislocations is seen in the coarse-grained sample (**Figure 6C**). In contrast, nano twins are well captured in the high pressure recovered nanocrystalline nickel, accompanied by some stacking faults⁴³ (**Figure 6A,B**). In short, twinning induced by stacking faults observed in the TEM measurements (**Figure 6**) originate from the nucleation and motion of partial dislocations¹⁵. This evidences that in the sub-10 nm particle size regime, the full-dislocation-mediated deformation shifts to the partial-dislocation-mediated deformation (with some degree of contribution of complete dislocation) in high-pressure compression.

FIGURE LEGENDS:

Figure 1: TEM and SEM images. TEM and SEM characterization of raw 3 nm (A), 8 nm (B), 12 nm (C), 20 nm (D), 40 nm (E), 70 nm (F), 100 nm (G), and 200 nm (H) nickel samples before compression. This figure has been adapted from Reference³⁶.

Figure 2: The experimental setup of radial DAC XRD. This figure has been adapted from Reference³⁶.

Figure 3: The top view of the sample chamber. The culet of the diamond needs to be smaller than the boron gasket (yellow part).

Figure 4: Azimuthally (0~360°) unrolled diffraction images of nickel at different pressures. The black arrows indicate the axial compression direction. At similar pressures, the curvature of diffraction lines increases with the decreasing grain size, suggesting the continuously mechanical strengthening. This figure has been adapted from Reference³⁶.

Figure 5: Size strengthening of nickel. From 200 nm to 3 nm, the nickel strengths (differential stress) always increase, reflecting the Hall-Petch relationship. This figure has been adapted from Reference³⁶.

Figure 6: TEM observations of representative nickel quenched from around 40 GPa. (A) 3 nm Ni. (B) 20 nm Ni. (C) 200 nm Ni. Partial dislocation-induced twins can be seen in nickel below 20 nm, while lots of perfect dislocation lines are observed in coarser grains. An edge dislocation (yellow "T") is labeled in the inset of (C).

DISCUSSION:

Computational simulations have been widely employed to study the grain size effect on the strength of nanometals^{5,6,16,17,27,42}. Perfect dislocations, partial dislocations, and GB deformation have been proposed to play decisive roles in the deformation mechanisms of the nanomaterials. In a molecular dynamics simulation, Yamakov et al.⁴² proposed a deformation mechanism map, including perfect dislocation, partial dislocation, and GB deformation, which depends on SF energy, the material's elastic properties, and the magnitude of the applied stress. Swygenhoven et al.²⁷ thought that slip in nano metals cannot be described in terms of the absolute value of SF energy but should be the generalized planar fault (GPF) energy involving stable and unstable SF energies. Jo et al.⁴³ found that different deformation modes, i.e., full slip, twinning, and SFs, are activated in different fcc metals by varying shear directions based on the GPF theory. These studies proposed that size softening would occur due to the dislocation-mediated to GB-mediated mechanism transition. However, these simulations cannot explain our observed size strengthening of sub-10 nm nickel nanocrystals. The current measurements indicate that the size strengthening is stronger in the smaller size range of nano nickel. Because perfect dislocations exist both in coarse- and fine-grained nickel, perfect dislocation cannot be the main strengthening reason. The slip of partial dislocations and the suppression of grain boundaries play an essential role in this extreme strengthening. The strength of the nano Pd and nano Au

using were also measured using the same approach. These results confirm that the size strengthening phenomenon in ultrafine-grained metals is universal with high-pressure suppression of grain boundary activities.

These results also emphasize the importance of radial DAC XRD experimentation^{14,38,44} in characterizing the mechanical performance of the nanomaterials. The high quality of large pieces (mm dimension and above) of real nanometer-grain-sized (below the critical grain size of 10 nm) metals is exceedingly difficult to manufacture because of grain coarsening and purity, even though severe plastic deformation (SPD) or equal channel angular pressing (ECAP) method. Therefore, there are few experimental mechanical measurements on sub-10 nm grained metals to reveal the strengthening phenomenon³⁰. Most inverse Hall-Petch relationship studies are reported by simulations⁶. The miniature tensile test requires a sample size of millimeter-level or above^{45,46}. This bulk geometry size of a millimeter (even sub mm, with the grain size below 10 nm sized polycrystalline metals, is hard to obtain their repeatable mechanical properties. Moreover, the mechanics of highly pure metal nano-powders cannot be measured directly by conventional approaches (tension or compression test). With synchrotron-based X-ray and radial DAC, the repeatable and reliable mechanical results of real nano-grain-sized (sub 10 nm) metal powders can be obtained. We firstly introduced rDAC XRD technique from geoscience to material science. This should be a significant breakthrough in the mechanical characterization of nanometals.

Compressive strength measurements with radial DAC XRD allow statistically examining the mechanical properties of even sub-10 nm grain-sized metals. The results are reproducible and reliable because of the excellent data statistics. This method would have more extended applications not only in geoscience but also in material science. Except for the advantages of the high-pressure radial DAC XRD techniques, they also have their limitations on strength measuring. They are usually used for powder or polycrystalline samples because of the established lattice strain theory³⁸. The high-pressure diffraction data of a single crystal is challenging to analyze. On the other hand, a non-hydrostatic high-pressure environment is needed to deform the samples, and the chamber is also small (<100 μm).

In summary, it was observed that other than the size softening in metals, known as the inverse Hall-Petch effect, the size strengthening can be extended down to 3 nm, much lower than that predicted by the established knowledge. Radial DAC XRD techniques are emphasized for evaluating the mechanical strength of the nanomaterials. The TEM observations reveal that the strengthening mechanisms shift from total dislocation-mediated plastic deformation to partial dislocation-associated plastic deformation. This finding encourages the efforts to achieve an even higher strength of materials by engineering grain sizes and grain boundary deformation suppression. This is expected to advance the industrial applications of nanometals further.

ACKNOWLEDGMENTS:

We acknowledge support from the National Natural Science Foundation of China (NSFC) under grant numbers 11621062, 11772294, U1530402, and 11811530001. This research was also partially supported by the China Postdoctoral Science Foundation (2021M690044). This research used the resources of the Advanced Light Source, which is a DOE Office of Science User Facility

under contract number DE-AC02-05CH11231 and the Shanghai Synchrotron Radiation Facility. This research was partially supported by COMPRES, the Consortium for Materials Properties Research in Earth Sciences under NSF Cooperative Agreement EAR 1606856.

DISCLOSURES:

The authors have nothing to disclose.

REFERENCES:

1. Hall, E. O. The Deformation and ageing of mild steel.3. Discussion of results. *Proceedings of the Physical Society of London Section B*. **64** (381), 747–753 (1951).
2. Conrad, H. Effect of grain size on the lower yield and flow stress of iron and steel. *Acta Metallurgica*. **11** (1), 75–77 (1963).
3. Kanninen, M. F., Rosenfield, A. R. Dynamics of dislocation pile-up formation. *The Philosophical Magazine: A Journal of Theoretical Experimental and Applied Physics*. **20** (165), 569–587 (1969).
4. Thompson, A. A. W. Yielding in nickel as a function of grain or cell size. *Acta Metallurgica*. **23** (11), 1337–1342 (1975).
5. Schiotz, J., Di Tolla, F. D., Jacobsen, K. W. Softening of nanocrystalline metals at very small grain sizes. *Nature*. **391** (6667), 561–563 (1998).
6. Schiotz, J., Jacobsen, K. W. A maximum in the strength of nanocrystalline copper. *Science*. **301** (5638), 1357–1359 (2003).
7. Conrad, H., Narayan, J. Mechanism for grain size softening in nanocrystalline Zn. *Applied Physics Letters*. **81** (12), 2241–2243 (2002).
8. Chokshi, A. H., Rosen, A., Karch, J., Gleiter, H. On the validity of the hall-petch relationship in nanocrystalline materials. *Scripta Metallurgica*. **23** (10), 1679–1683 (1989).
9. Sanders, P. G., Eastman, J. A., Weertman, J. R. Elastic and tensile behavior of nanocrystalline copper and palladium. *Acta Materialia*. **45** (10), 4019–4025 (1997).
10. Conrad, H., Narayan, J. On the grain size softening in nanocrystalline materials. *Scripta Materialia*. **42** (11), 1025–1030 (2000).
11. Chen, J., Lu, L., Lu, K. Hardness and strain rate sensitivity of nanocrystalline Cu. *Scripta Materialia*. **54** (11), 1913–1918 (2006).
12. Knapp, J. A., Follstaedt, D. M. Hall–Petch relationship in pulsed-laser deposited nickel films. *Journal of Materials Research*. **19** (1), 218–227 (2004).
13. Kumar, K. S., Suresh, S., Chisholm, M. F., Horton, J. A., Wang, P. Deformation of electrodeposited nanocrystalline nickel. *Acta Materialia*. **51** (2), 387–405 (2003).
14. Chen, B. et al. Texture of nanocrystalline nickel: Probing the lower size limit of dislocation activity. *Science*. **338** (6113), 1448–1451 (2012).
15. Chen, M. W. et al. Deformation twinning in nanocrystalline aluminum. *Science*. **300** (5623), 1275–1277 (2003).
16. Yamakov, V., Wolf, D., Phillpot, S. R., Gleiter, H. Deformation twinning in nanocrystalline Al by molecular-dynamics simulation. *Acta Materialia*. **50** (20), 5005–5020 (2002).
17. Yamakov, V., Wolf, D., Phillpot, S. R., Mukherjee, A. K., Gleiter, H. Dislocation processes in the deformation of nanocrystalline aluminium by molecular-dynamics simulation. *Nature Materials*. **1** (1), 45–49 (2002).

- 438 18. Yamakov, V., Wolf, D., Salazar, M., Phillpot, S. R., Gleiter, H. Length-scale effects in the
439 nucleation of extended dislocations in nanocrystalline Al by molecular-dynamics simulation. *Acta*
440 *Materialia*. **49** (14), 2713–2722 (2001).
- 441 19. Shan, Z. W. et al. Grain boundary-mediated plasticity in nanocrystalline nickel. *Science*.
442 **305** (5684), 654–657 (2004).
- 443 20. Li, H. et al. Strain-dependent deformation behavior in nanocrystalline metals. *Physical*
444 *Review Letters*. **101** (1), 015502 (2008).
- 445 21. Van Swygenhoven, H., Derlet, P. M. Grain-boundary sliding in nanocrystalline fcc metals.
446 *Physical Review B*. **64** (22), 224105 (2001).
- 447 22. Ovid'ko, I. A. Deformation of nanostructures. *Science*. **295** (5564), 2386 (2002).
- 448 23. Murayama, M., Howe, J. M., Hidaka, H., Takaki, S. Atomic-level observation of disclination
449 dipoles in mechanically milled, nanocrystalline Fe. *Science*. **295** (5564), 2433 (2002).
- 450 24. Wang, L. et al. Grain rotation mediated by grain boundary dislocations in nanocrystalline
451 platinum. *Nature Communications*. **5**, 4402 (2014).
- 452 25. Edalati, K. et al. Influence of dislocation–solute atom interactions and stacking fault
453 energy on grain size of single-phase alloys after severe plastic deformation using high-pressure
454 torsion. *Acta Materialia*. **69**, 68–77 (2014).
- 455 26. Edalati, K., Horita, Z. High-pressure torsion of pure metals: Influence of atomic bond
456 parameters and stacking fault energy on grain size and correlation with hardness. *Acta*
457 *Materialia*. **59** (17), 6831–6836 (2011).
- 458 27. Yamakov, V., Wolf, D., Phillpot, S. R., Mukherjee, A. K., Gleiter, H. Deformation-
459 mechanism map for nanocrystalline metals by molecular-dynamics simulation. *Nature Materials*.
460 **3** (1), 43–47 (2004).
- 461 28. Starink, M. J., Cheng, X., Yang, S. Hardening of pure metals by high-pressure torsion: A
462 physically based model employing volume-averaged defect evolutions. *Acta Materialia*. **61** (1),
463 183–192 (2013).
- 464 29. Yang, T. et al. Ultrahigh-strength and ductile superlattice alloys with nanoscale disordered
465 interfaces. *Science*. **369** (6502), 427 (2020).
- 466 30. Hu, J., Shi, Y. N., Sauvage, X., Sha, G., Lu, K. Grain boundary stability governs hardening
467 and softening in extremely fine nanograined metals. *Science*. **355** (6331), 1292 (2017).
- 468 31. Yue, Y. et al. Hierarchically structured diamond composite with exceptional toughness.
469 *Nature*. **582** (7812), 370–374 (2020).
- 470 32. Li, X. Y., Jin, Z. H., Zhou, X., Lu, K. Constrained minimal-interface structures in
471 polycrystalline copper with extremely fine grains. *Science*. **370** (6518), 831 (2020).
- 472 33. Yan, S. et al. Crystal plasticity in fusion zone of a hybrid laser welded Al alloys joint: From
473 nanoscale to macroscale. *Materials & Design*. **160**, 313–324 (2018).
- 474 34. Khalajhedayati, A., Pan, Z., Rupert, T. J. Manipulating the interfacial structure of
475 nanomaterials to achieve a unique combination of strength and ductility. *Nature*
476 *Communications*. **7** (1), 10802 (2016).
- 477 35. Chen, L. Y. et al. Processing and properties of magnesium containing a dense uniform
478 dispersion of nanoparticles. *Nature*. **528** (7583), 539–543 (2015).
- 479 36. Zhou, X. et al. High-pressure strengthening in ultrafine-grained metals. *Nature*. **579**
480 (7797), 67–72 (2020).
- 481 37. Lutterotti, L., Vasin, R., Wenk, H.-R. Rietveld texture analysis from synchrotron diffraction

- images. I. Calibration and basic analysis. *Powder Diffraction*. **29** (1), 76–84 (2014).
38. Singh, A. K., Balasingh, C., Mao, H. K., Hemley, R. J., Shu, J. F. Analysis of lattice strains measured under nonhydrostatic pressure. *Journal of Applied Physics*. **83** (12), 7567–7575 (1998).
39. Hemley, R. J. et al. X-ray imaging of stress and strain of diamond, iron, and tungsten at megabar pressures. *Science*. **276** (5316), 1242–1245 (1997).
40. Merkel, S. et al. Deformation of polycrystalline MgO at pressures of the lower mantle. *Journal of Geophysical Research-Solid Earth*. **107** (B11), 2271 (2002).
41. Singh, A. K. The lattice strains in a specimen (cubic system) compressed nonhydrostatically in an opposed anvil device. *Journal of Applied Physics*. **73** (9), 4278–4286 (1993).
42. Van Swygenhoven, H., Derlet, P. M., Frøseth, A. G. Stacking fault energies and slip in nanocrystalline metals. *Nature Materials*. **3** (6), 399–403 (2004).
43. Jo, M. et al. Theory for plasticity of face-centered cubic metals. *Proceedings of the National Academy of Sciences of the United States of America*. **111** (18), 6560 (2014).
44. Chung, H. Y. et al. Synthesis of ultra-incompressible superhard rhenium diboride at ambient pressure. *Science*. **316** (5823), 436–439 (2007).
45. Klueh, R. L. Miniature tensile test specimens for fusion reactor irradiation studies. *Nuclear Engineering and Design. Fusion*. **2** (3), 407–416 (1985).
46. Konopík, P., Farahnak, P., Rund, M., Džugan, J., Rzepa, S. Applicability of miniature tensile test in the automotive sector. *IOP Conference Series: Materials Science and Engineering*. **461**, 012043 (2018).

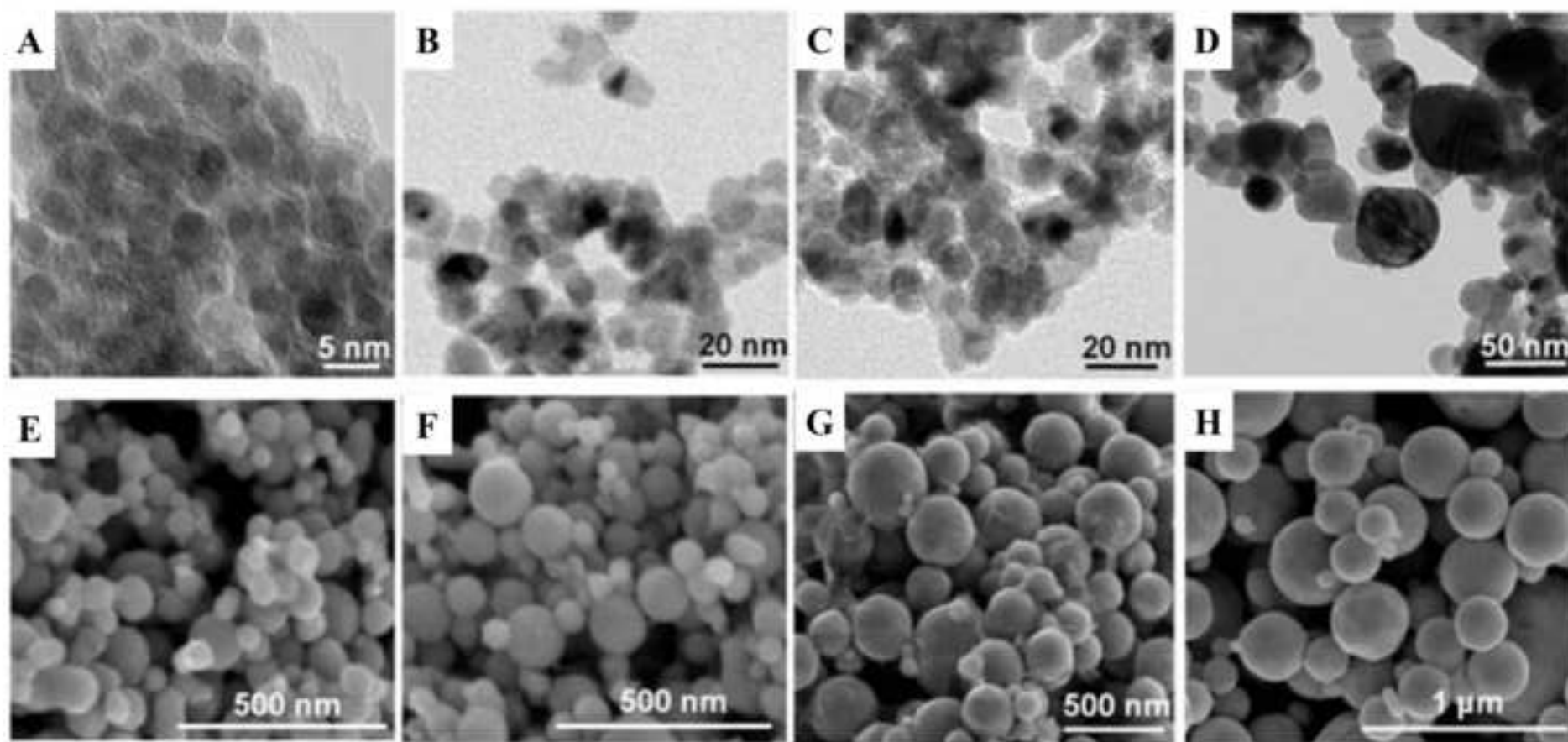
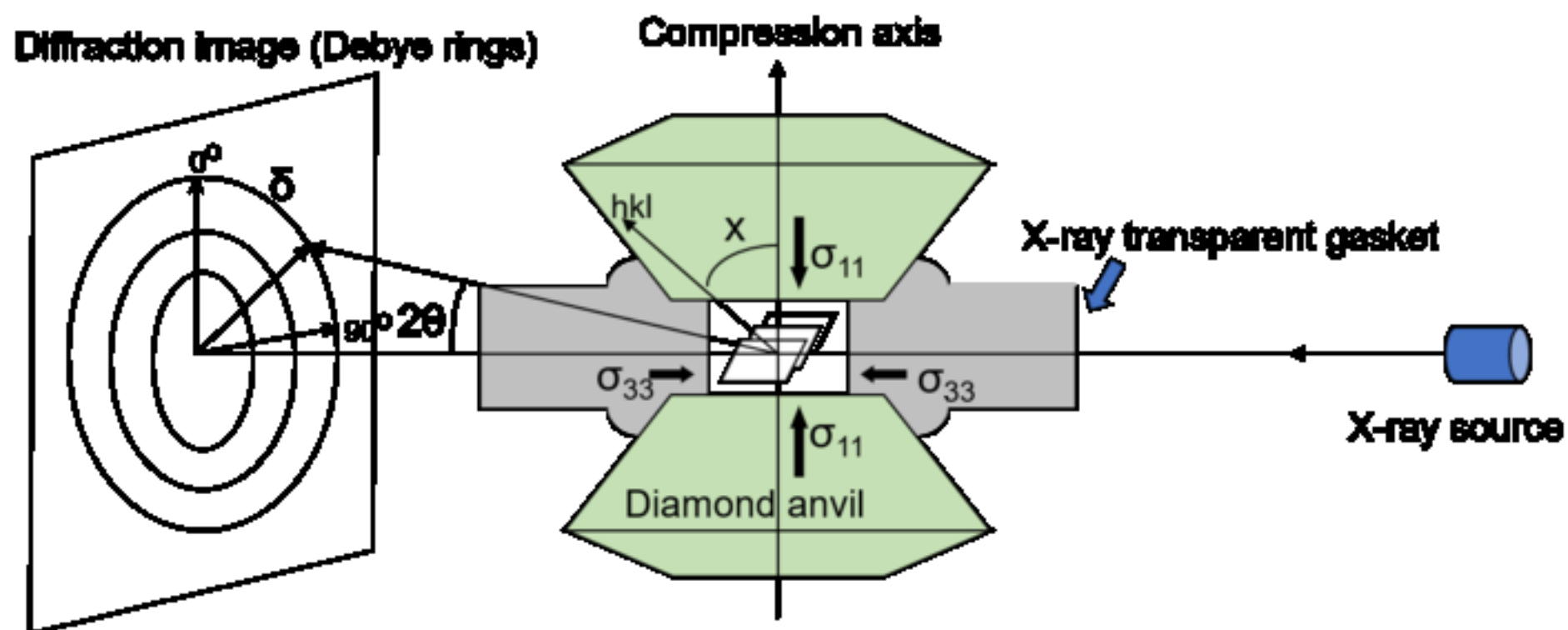


Figure 2



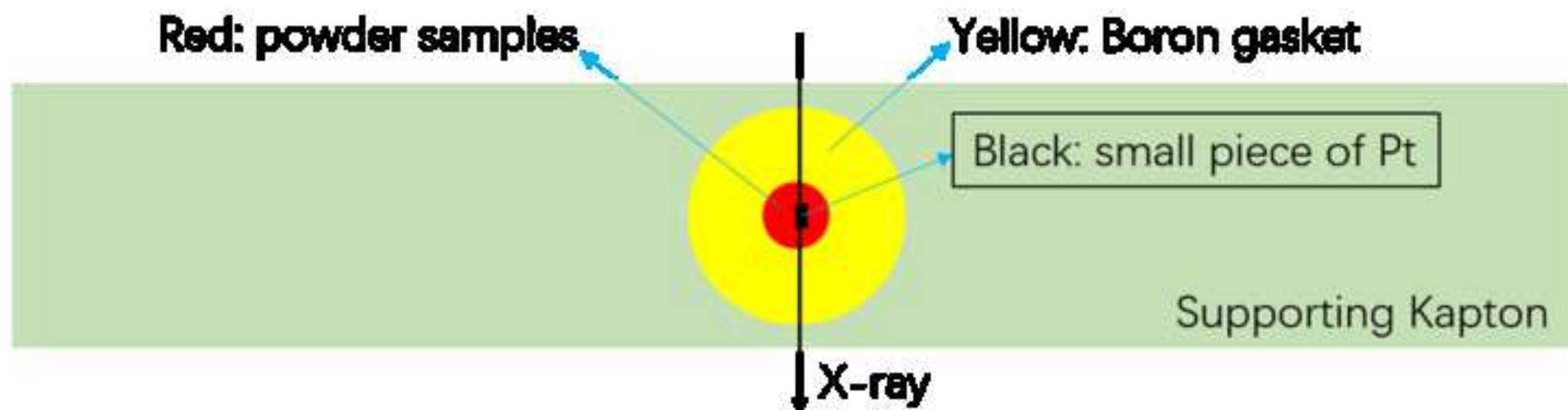


Figure 4

[Click here to access/download;Figure;Figure 4_revised.tif](#)

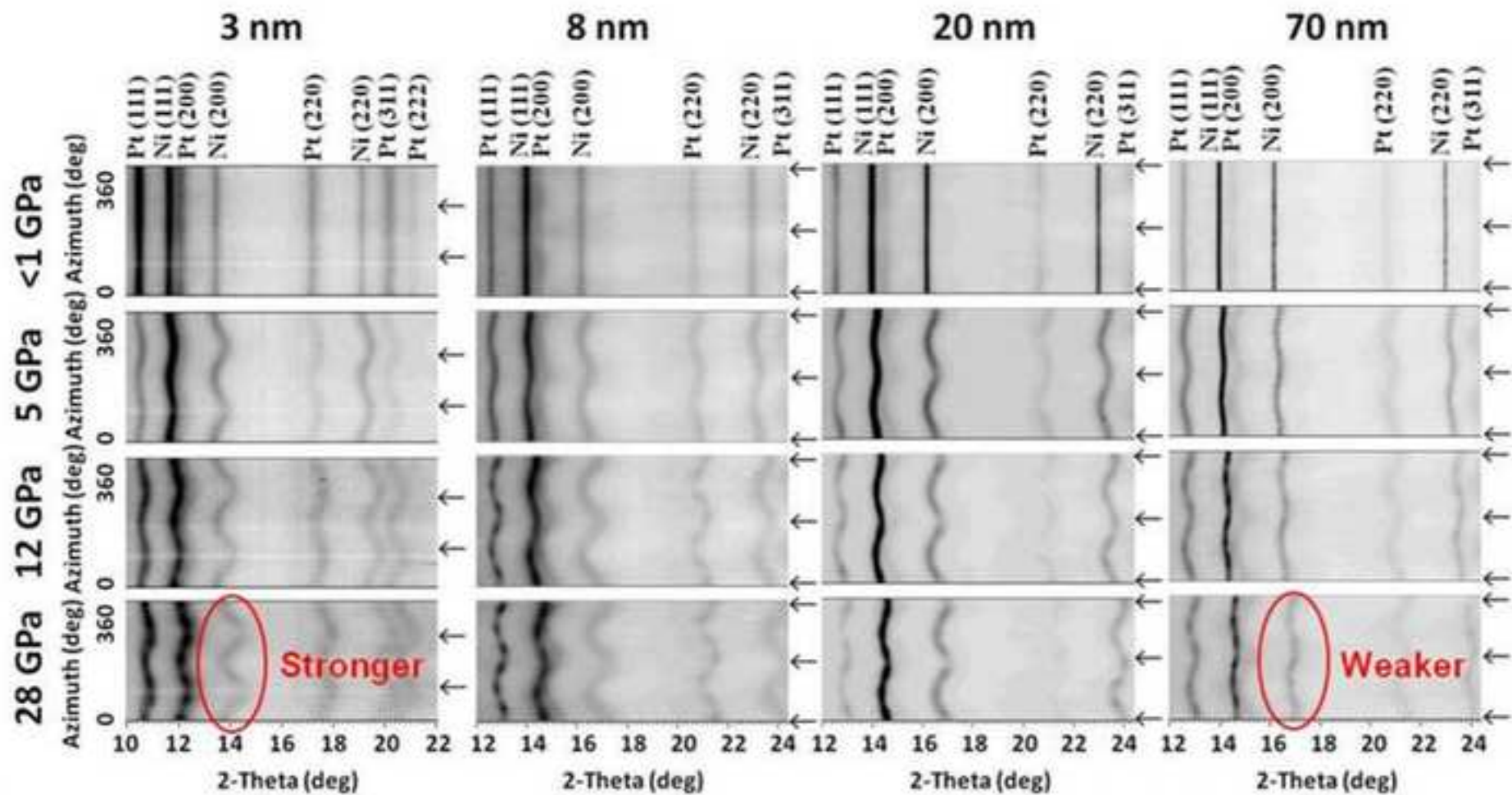
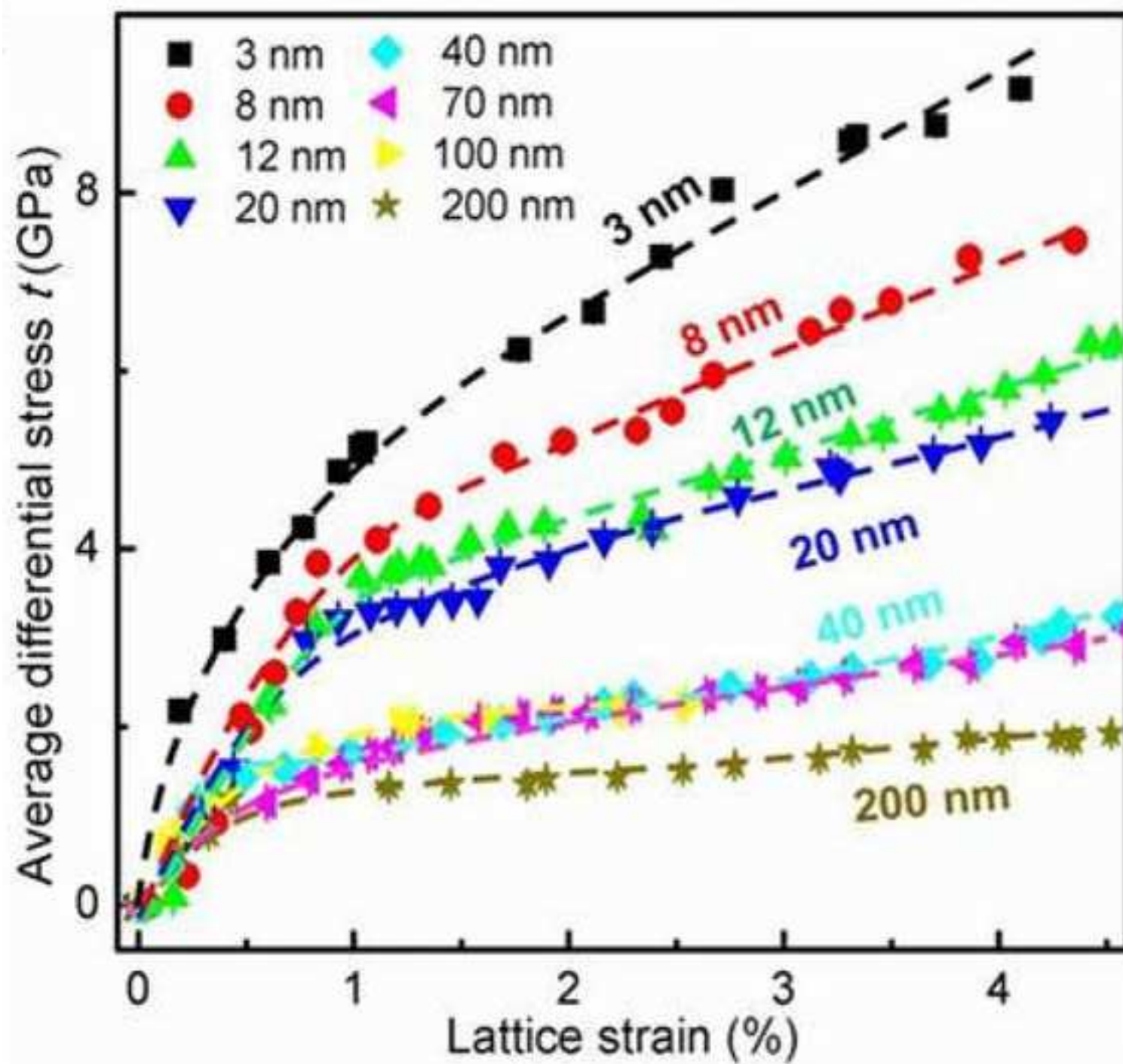
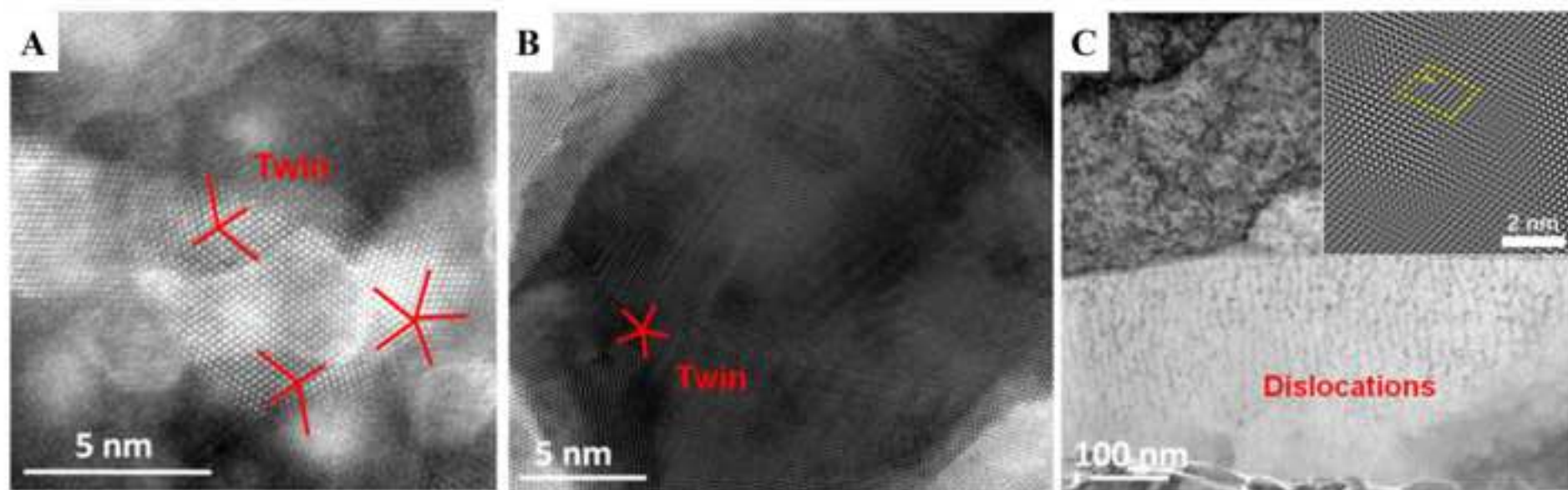


Figure 5







[Click here to access/download](#)

Table of Materials
61819_R2_Table of Materials.xlsx



Rebuttal Letter

Journal of Visualized Experiments
Editorial Office

October 4, 2021

Dear Editor:

We are re-submitting a manuscript entitled “Determining the mechanical strength of ultra-fine-grained metals” for your consideration as to its suitability for publication in Journal of Visualized Experiments. None of the material has been published or under consideration elsewhere, including the Internet.

We have revised the manuscript according to your and the reviewers’ suggestions. We rewrote the Summary and Protocol parts; deleted the EVPSC simulation part; added more figures and discussions, etc. We summarized the responses to the comments of you and the reviewers in the response letter.

Most of the mechanisms of Hall-Petch or inverse Hall-Petch effects are discussed in ambient pressure. We have interpreted our results more carefully and clearly.

- 1) Traditional experimental methods do not apply to the materials of ultrafine nanoparticles.
- 2) We have extrapolated our high-pressure strengthening results to ambient pressure for more straightforward comparison.

Therefore, our results are reliable. We hope that we have clarified the advantages and disadvantages of our approach for determining the mechanical strength of ultra-fine-grained metals (line 306-312).

If you have any questions, please do not hesitate to contact us:

Tel: +86(21)80177063,

Fax: +86(21)80177064,

E-mail: chenbin@hpstar.ac.cn

Sincerely,

Bin Chen

Center for High Pressure Science & Technology Advanced Research, Shanghai, China

Authors' Responses to the Reviewers

(Manuscript # JoVE61819)

Editorial comments:

1. Please take this opportunity to thoroughly proofread the manuscript to ensure that there are no spelling or grammar issues.

Authors' Response >> Thanks for the reminding. We have done the checking and corrections.

2. Please rephrase the Summary to clearly describe the protocol and its applications in complete sentences between 10-50 words: "Here, we present a protocol to ..."

Authors' Response >> We have rephrased the Summary as "Here, we present a protocol to conduct the high-pressure radial diamond-anvil-cell experiments and analyze the related data, which are important to obtain mechanical strength of nanomaterials with a big breakthrough to traditional approach."

3. Unfortunately, there are sections of the manuscript that show overlap with previously published work. Please revise lines: 49-52, 189-190, 198-202, 234-240, 247-250, 258-261, 270-279, 340-344, 347-350, 351-354.

Authors' Response >> We have deleted or restated the relevant parts mentioned above.

4. Please add more details to your protocol steps. Please ensure you answer the "how" question, i.e., how is the step performed? Alternatively, add references to published material specifying how to perform the protocol action. For example, in 1.2.1, how much ethanol is to be used, and how is the 8 nm nickel powder to be obtained? How is TEM to be performed to check size distribution?

Authors' Response >> We have rewritten part of the protocol and added more details in the updated manuscript.

5. The Protocol should contain only action items that direct the reader to do something. Please move the discussion about the protocol to the Discussion or rewrite the protocol

to answer the “how” question, i.e., how is the step performed? Alternatively, add references to published material specifying how to perform the protocol action. The Protocol should be made up almost entirely of discrete steps without large paragraphs of text between sections.

Authors’ Response >> We have rewritten parts of the Protocol, and deleted some unimportant parts.

6. In the discussion, please discuss limitations of the method.

Authors’ Response >> We have discussed the limitation of the method in “DISCUSSION part” as following: “Except for the advantages of the high-pressure radial DAC XRD techniques, they also have their limitations on strength measuring. They are usually used for powder or polycrystalline samples because of the established lattice strain theory. The high-pressure diffraction data of single crystal is very difficult to analyze. In the other hand, we need non-hydrostatic high-pressure environment to deform the samples, then the chamber is small (usually less than 100 micron).”

Reviewers' comments:

Reviewer #1:

The manuscript deals with determination of the strength of ultrafine-grained materials using X-ray diffraction in the diamond anvil cell (DAC) experiments. Employment of DAC to evaluate the strength is interesting, but the authors need to make their conclusions and discussion by care because the high hydrostatic pressure in DAC significantly influence the deformation mechanism. Discussion about the Hall-Petch or inverse Hall-Petch mechanisms are usually made under low hydrostatic pressure (atmospheric pressure). In addition to this general comment, some other comments are given below.

Authors’ Response >> Thanks. Yes, most of the mechanisms of Hall-Petch or inverse Hall-Petch effects are discussed in ambient pressure. We should interpret our results more carefully and clearly.

1) Traditional experimental methods do not apply to the materials of ultrafine nanoparticles.

2) We have extrapolated our high-pressure strengthening results to ambient pressure for more straightforward comparison.

- The TEM results should be provided for all samples to confirm the reliability of grain sizes. The authors commented about dislocations in Fig. 5, but it is hard to see the dislocations in the PDF file. A better quality is required.

Authors' Response >> The TEM images about the original samples have added to confirm the grain sizes in the updated manuscript (Fig. 1). A high resolution TEM image is added in Fig. 6c.

- The authors' comments "However, evaluation of strength by tensile loading is often technically difficult for nanograined metals of especially sub-10 nm grain sizes as the premature fracture may occur before the flow stress reaches the ultimate tensile strength." is not so correct because miniature tensile test is used very often to examine ultra-fine grained materials.

Authors' Response >> Thanks. We would appreciate if referees would provide the information of related literature. As we know, it is technically difficult to hold fine nanoparticles for tensile strength measurements while the measurements for bulk volume nanomaterials cannot effectively exclude the effects of grain boundaries. Most inverse Hall-Petch relationship studies are simulation studies(Schiotz, J. et al. Science 301 1357-1359, 2003). Miniature tensile test requires the sample size of millimeter-level or above ([https://doi.org/10.1016/0167-899X\(85\)90028-X](https://doi.org/10.1016/0167-899X(85)90028-X), <https://iopscience.iop.org/article/10.1088/1757-899X/461/1/012043>). Making such bulk geometry size of millimeter (even sub-mm, with the grain size below 10 nm sized polycrystalline metals is another big challenge in materials science and engineering.

- It is hard to accept the third sentence in the abstract: "However, characterizing the strength of materials at the lower nanometer scale has been a big challenge as the traditional techniques (tension or indentation test, etc.) become no longer effective and reliable."

Authors' Response >> Sorry that our knowledge is that characterizing the strength (and deformation mechanisms) of nanometals is still a big challenge up to now. We would appreciate if referees would provide the information of some related literature.

- Did the authors try to validate their modeled strength by using other standard methods?

Authors' Response >> Yes, we conducted a series of strength measurements by rDAC with the particle size from millimeter to 3 nm. The strength results of coarse-grained nickel are comparable to those from traditional tests (Vickers indentation test etc.). So, we believe the strength results from rDAC is acceptable and reasonable.

- Details of materials and experiments should be given so that independent researchers can conduct the same experiments.

Authors' Response >> We have put the materials' details (Protocol 1 and Fig. 1) and experimental details (Protocol 2.3) in the updated manuscript. The setup (Figs. 2-3) is not complicated, and the sample is pure nano metal powders. The strength results have good repeatability. So, this method is reliable.

- Unlike the claim of authors in the introduction, there have been significant activities on strength of ultrafine-grained materials and underlying mechanisms. The authors are referred to the works by materials scientists such as

Nature Materials, Vol. 3, pp. 511-516, 2004.

Acta Materialia, Vol. 59, No. 17, pp. 6831-6836, 2011.

Acta Materialia, Vol. 61, No. 1, pp. 183-192, 2013

Acta Materialia, Vol. 69, No. 8, pp. 68-77, 2014.

Authors' Response >> Thanks. We have added these literatures into our references. We note that the grain size of nanomaterials in these studies is above 10 nm.

- The authors should note that not all nonmetals exhibit inverse Hall-Petch effect. Please search this issue for nickel and add some details and references to the introduction.

Authors' Response >> Agree. We have mentioned both Hall-Petch and inverse Hall-Petch relationship in the introduction part. The key point of softening or not is mainly the grain boundary activities (diffusion or sliding). More discussion is added.

Reviewer #2:

Manuscript Summary:

The authors employed the radial diamond anvil cell method in conjunction with X-Ray diffraction at a commercial beamline to monitor the changes in the physical characteristics of nanomaterials in order to determine the strength of ultrafine metals.

Major Concerns:

I do not have any major concerns. This manuscript can be published once the authors

respond to the minor concerns raised by me.

Authors' Response >> Thanks.

Minor Concerns:

There are several incomplete sentences in the Abstract; "overcomes the limitations of traditional methods"...such as? ; "reliable characterizing techniques....?"

Authors' Response >> We have revised these as following: "However, characterizing the strength of materials at the lower nanometer scale has been a big challenge, because the traditional techniques (tension or indentation test, etc.) become no longer effective and reliable, such as nano-indentation test, micropillar compression test, tensile test, etc."

Introduction, line 68, please provide a list of traditional methods that have been employed to measure the strength of nanometals along with references.

Authors' Response >>The conventional methods to measure the strength are tensile test, Vickers hardness test, nano-indentation test, micropillar test, etc. (Ref.29-35). We have updated these references in the manuscript.

Has this method been previously used to measure the strengths and deformation texturing? If yes, please provide appropriate references along with which metals or alloys were investigated.

Authors' Response >> Yes, this method has been employed to examine the strength and deformation texturing of materials, such as ReB₂ (H.Y. Chung, et al. Science 316 436-439, 2007), nano Ni (B. Chen, et al. Science 338, 1448-1451, 2012), Fe (W.L. Mao et al. J. Geophys. Res. 113, B09213, 2008), etc.

The authors have not cited several seminal papers in this field such as the 1993 paper by Wu and Bassett.

Authors' Response >> Thanks. Added as suggested (Ref.36).

Protocol section; please provide the country where the chemical companies are located.

Authors' Response >>These three chemical companies mentioned in protocol are all in USA. We have stated them in updated main text.

Please provide more information regarding the optimization of the setup.

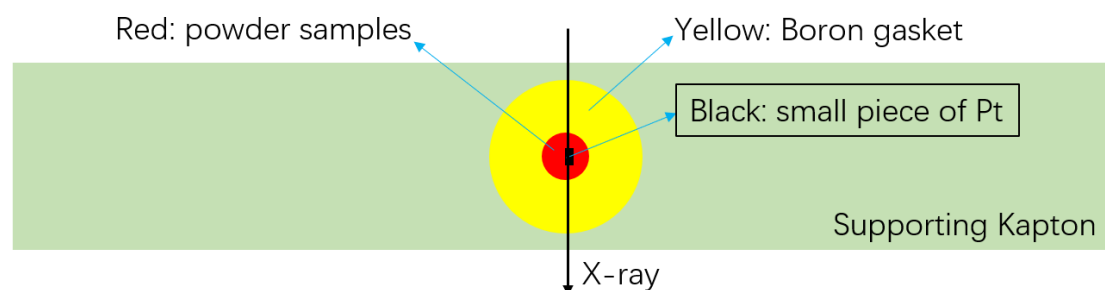
Authors' Response >> Here are the details of our setup (Protocol 2.3 and Figs. 2-3): X-ray transparent boron-Kapton gaskets with a thickness of 80 μm and a sample chamber of 60 μm diameter was mounted on top of 300 μm culet DAC with the support of clays (the size of the supporting Kapton is 8 mm in long and 1.5 mm in width). Ni powders were pre-compacted before being loaded into the sample chamber. A small piece of Pt foil was placed on top of the Ni sample to serve as a pressure calibrant using the Birch-Murnaghan equation of state of Pt. No pressure medium was used in order to maximize the differential stress between axial and radial directions. Monochromatic synchrotron x-rays with energies of 30 keV (for 3 nm Ni sample) or 25 keV (for other Ni samples) were used to conduct the XRD experiments at beamline 12.2.2 of the Advanced Light Source, Lawrence Berkeley National Lab. The experimental setup is shown in Figure 1. A Mar345 detector with the resolution of 100 μm /pixel was used to collect the diffraction images. CeO_2 or LaB_6 standard were used to calibrate the instrumental parameters.

Plots of distribution of deviatoric stress as a function of radial distance will be helpful for known samples.

Authors' Response >> Because the X-ray penetrate the whole sample through the center (like Fig. 3) and the sample size is really small, we cannot plot the deviatoric stress as a function of radial distance.

Can the authors provide a top down view of the sample in the high pressure chamber?

Authors' Response >> The top down view is as the following schematic drawing (Figure 3 in the main text).



Line 132, what is Z?

Authors' Response >> Z represents atomic number (low Z means light element). We have changed “Z” to “atomic number” in the main text.

What kind of laser drilling machine was used? Please provide specifications.

Authors' Response >> We have a commercial 532 nm laser milling machine from Oxford Instruments specialized for cutting accurate small diameter very round holes in typical DAC gasket materials.

RE: obtain explicit copyright permission to reuse 3 figures from nature publication

发件人: **Journalpermissions** <journalpermissions@springernature.com>
收件人: Jianing Xu_许家宁 <jianing.xu@hpstar.ac.cn>
抄 送: Bin Chen_陈斌 <chenbin@hpstar.ac.cn>
时 间: 2021年10月27日(星期三) 00:35

Dear Jianing,

Thank you for your email.

Springer Nature journal authors are free to reproduce, or allow a third party to reproduce, their published article in whole or in part, in any other type of work written by the Author, and after an embargo period of 12 months. Any such reuse should provide a clear citation to the original publication according to any standard referencing system, which at a minimum should include "Journal name, volume, page number, year, Springer Nature"

As the embargo period has passed for your article, you are free to reuse this work in your new publication.

If you need a formal licence, please search for your article on link.springer.com or nature.com. At the end of the article page, click on the "Rights and Permissions" tab to be redirected to our CCC RightsLink service where you may input the details of your request. Please be sure to tick the box that asks whether you are the author on the order entry page.

Best wishes,

Bod

Bod Adegboyega

Permissions Assistant

Springer Nature

4 Crinan Street, London N1 9XW, UK

T +44 (0) 442034263235

Bod.adegboyega.1@springernature.com

From: Jianing Xu_许家宁 <jianing.xu@hpstar.ac.cn>

Sent: 11 October 2021 13:32

To: Journalpermissions <journalpermissions@springernature.com>

Cc: Bin Chen_陈斌 <chenbin@hpstar.ac.cn>

Subject: obtain explicit copyright permission to reuse 3 figures from nature publication

[External - Use Caution]

Dear Nature editor,

Our group published one nature paper entitled "High-pressure strengthening in ultrafine-grained metals" last year. The on-line link is "<https://www.nature.com/articles/s41586-020-2036-z>".

Now, we would like to publish the related experimental methodology in Journal of Visualized Experiments (JoVE, a video journal), and will reuse the **Fig. 1, Extended Data Fig. 1, and Extended Data Fig. 3** from this nature paper. As per JoVE's policy, we need explicit copyright permission from the respective journal for reusing any previously published figures/tables.

Can we have the reuse permission (3 Figures) from nature if possible?

Thank you,

Jianing

Co-first author of this Nature paper

Jianing Xu, Ph. D.

Center for High Pressure Science & Technology Advanced Research (HPSTAR)

Bldg 6,1690 Cailun Rd, Pudong, Shanghai 201203

Tel: +86-13240774207

Email: jianing.xu@hpstar.ac.cn

Website: <http://hpstar.ac.cn/channels/115.html>

北京高压科学研究中心 中国-上海 201203
